Assessing the Errors from Dimensional Splitting in a 3D Discontinuous Galerkin Atmospheric Model

Ram D. Nair

Institute for Mathematics Applied to Geosciences (IMAGe)
Computational Information Systems Laboratory

National Center for Atmospheric Research, Boulder, CO 80305, USA.

François Hébert

Cornell University, Ithaca, New York, USA.

[AGU Fall Meeting, San Francisco, 14th December, 2016.]

3D Atmospheric Modeling

Traditionally, atmospheric model treats the horizontal (2D) and vertical (1D) dimensions separately.

- Large aspect ratio between horizontal vertical grid spacing ($\approx 1 : O(100)$)
- 'Special treatment' for the vertical dynamics
- Facilitate implementation of efficient "HEVI-type" time integration schemes.
- In general, splitting method based on temporal or spatial, can introduce 'split errors'

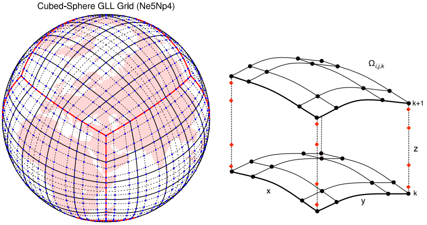

Nair, Bao & Toy (AIAA, 2016)

New generation non-hydrostatic models based on high-order Galerkin methods such as the spectral element (SE) and discontinuous Galerkin (DG), gaining popularity

- Full-3D: NUMA, Giraldo et al. (2013); Blaise et al. (2015) use 3D hexahedral elements.
- Split (2D+1D): HOMME, CAM-SE, KIAPS. SE/DG horizontal + 1D FD/H-O vertical

What errors are introduced by dimension-splitting in a 3D DG model?

DG Formulation: Atmospheric Conservation Laws

- Atmospheric equations of motion in 3D Cartesian (x,y,z) coordinates can be written in the general flux-from:

$$\frac{\partial U}{\partial t} + \nabla \cdot \mathbf{F}(U) \equiv \frac{\partial U}{\partial t} + \frac{\partial}{\partial x}F_1(U) + \frac{\partial}{\partial y}F_2(U) + \frac{\partial}{\partial z}F_3(U) = S(U)$$

U is the conservative variable, $\mathbf{F} = (F_1, F_2, F_3)$ is the flux function and $S(U)$ is the source term.

- E.g: For a transport equation $U = \rho$, a scalar; for the Euler system $U = [\rho, \rho u, \rho v, \rho w, \rho\theta]^T$
- Split 2D + 1D: The 3D Eqn. is split into the horizontal (x,y) and vertical z directions.

$$\frac{\partial U}{\partial t} + \nabla_{2d} \cdot \mathbf{F}(U) \equiv \frac{\partial U}{\partial t} + \frac{\partial}{\partial x}F_1(U) + \frac{\partial}{\partial y}F_2(U) = -\frac{\partial}{\partial z}F_3(U) + S(U)$$

- Discontinuous Galerkin Formulation – Common Steps:

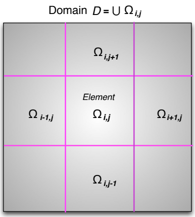

- The domain $\mathscr{D}$ is partitioned into non-overlapping elements Ω_e. Element edges are discontinuous
- Approximate solution U_h belongs to a vector space $\mathscr{V}_h$ of polynomials $\mathscr{P}_N(\Omega_e)$.
- Galerkin formulation is obtained by multiplying the basic equation by a *test function* $\varphi_h \in \mathscr{V}_h$ and integration over an element Ω_e

$$\int_{\Omega_e} \left[\frac{\partial U_h}{\partial t} + \nabla \cdot \mathbf{F}(U_h) - S(U_h) \right] \varphi_h \, d\Omega = 0$$

- Discontinuity at the element edges is resolved by Lax-Friedrichs numerical flux.

DG Discretization

- For full 3D elements, the weak Galerkin formulation is obtained from:

$$\int\int\int_{\Omega_e} \left[\frac{\partial U_h}{\partial t} + \nabla \cdot \mathbf{F}(U_h) - S(U_h) \right] \varphi_h d\Omega = 0$$

- For the split 2D+1D case,

$$\int\int_{\Omega_e} \left[\frac{\partial U_h}{\partial t} + \nabla_{2d} \cdot \mathbf{F}(U_h) - \tilde{S}(U_h) \right] \varphi_h d\Omega = 0, \quad \tilde{S}(U) = -\frac{\partial}{\partial z} F_3(U) + S(U)$$

- The vertical 1D flux derivative $\partial F_3(U)/\partial z$ can be discretized by any numerical method, including 1D DGM.
- Evaluation of the integrals:

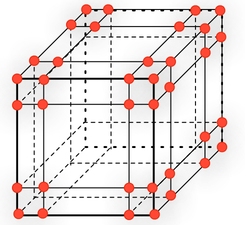

3D GLL Grid Box

- Ω_e is mapped onto high-order quadrature element $Q = [-1,1]^d$
- Gauss-Lobatto-Legendre (GLL) quadrature is efficient
- A tensor-product of Lagrange basis functions $(h_l(\xi), \xi \in [-1,1])$ of order N represents the approximate solution on Q. In 3D case:

$$U_h(\xi^1, \xi^2, \xi^3) = \sum_{i=0}^{N} \sum_{j=0}^{N} \sum_{k=0}^{N} U_{ijk}\, h_i(\xi^1)\, h_j(\xi^2)\, h_k(\xi^3)$$

- Spatial discretization leads to the ODE

$$\frac{dU_h}{dt} = \mathscr{L}(U_h)$$

- For our implementation, SSP-RK3 explicit ODE solver is used.

3D Advection Test: Smooth Solid-Body Rotation

To Solve:

$$\frac{\partial \rho}{\partial t} + \frac{\partial \rho u}{\partial x} + \frac{\partial \rho v}{\partial y} + \frac{\partial \rho w}{\partial z} = 0$$

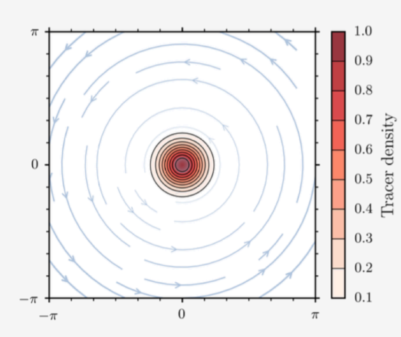

x-z slice through simulation domain

- Physical domain: $[-\pi, \pi]^3$
- Solid-body rotation with $u = -(z - z_0)$, $v = 0$ and $w = (x - x_0)$.
- BC: Lateral - Periodic; Top/Bottom - Periodic
- The Gaussian blob centered at the domain center (x_0, y_0, z_0),

$$\rho(x,y,z) = a \exp[-r^2/(2\sigma^2)]$$

with $r^2 = (x-x_0)^2 + (y-y_0)^2 + (z-z_0)^2$, $a = 1$, $\sigma = 0.35$.

- Period for one revolution $t = 2\pi$

- DG simulations with full 3D and split 2D+1D. Starting with $8 \times 8 \times 8$ elements, and 4^3 GLL points on each element.

3D Advection Test: Smooth Solid-Body Rotation

- The full 3D and split 2D+1D results match expected h/p-convergence rate

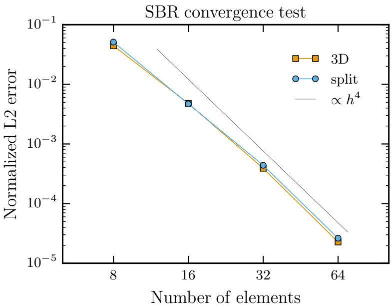

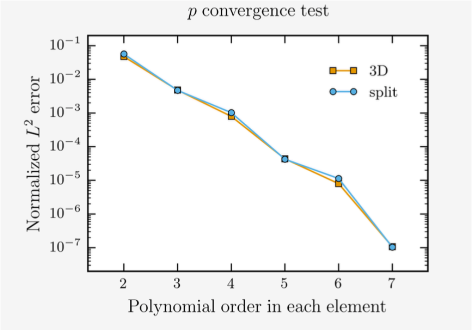

3D Advection Test: Deformational Flow (multi-scale)

- Initial fields (double Gaussian) stretched into thin filaments, the flow reverses and return to the initial state (Nair & Lauritzen, JCP, 2010).
- Domain : $[0,2\pi]\times[0,\pi]\times[0,\pi]$. Final time $T=5$ units
- Initial density $\rho(x,y,z)$ centered at $\mathbf{x}_1=(5\pi/6,\pi/2,\pi/2)$, $\mathbf{x}_2=(7\pi/6,\pi/2,\pi/2)$

$$\rho(x,y,z)=a\left[\exp\left(-\frac{|\mathbf{x}-\mathbf{x}_1|^2}{b}\right)+\exp\left(-\frac{|\mathbf{x}-\mathbf{x}_2|^2}{b}\right)\right],\quad a=0.95,\, b=0.2$$

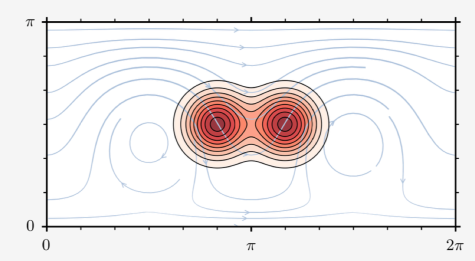

Initial fields $\rho(x,y,z)$ in x-z plane

- Time dependent non-divergent velocity fields

$$u(x,y,z)=u_0\sin^2\left[2\pi\left(\frac{x}{2\pi}-\frac{t}{T}\right)\right]\sin\left[2\pi\left(\frac{z}{\pi}\right)\right]\times\cos\left(\frac{\pi t}{T}\right)+\frac{2\pi}{T}$$

$$v(x,y,z)=0$$

$$w(x,y,z)=w_0\sin\left[4\pi\left(\frac{x}{2\pi}-\frac{t}{T}\right)\right]\sin^2\left[\pi\left(\frac{z}{\pi}\right)\right]\times\cos\left(\frac{\pi t}{T}\right)$$

Deformational Flow: h Convergences

-

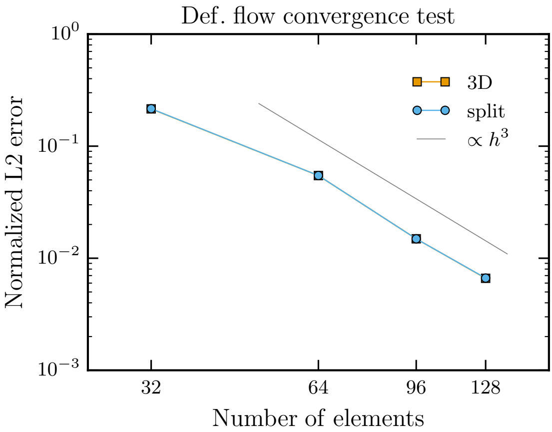

Flow over a 3D mountain Test: $(x, y, z) \to (x, y, \zeta)$

- Terrain-following vertical coordinate transformation (Gal-Chen & Somerville, JCP 1975)

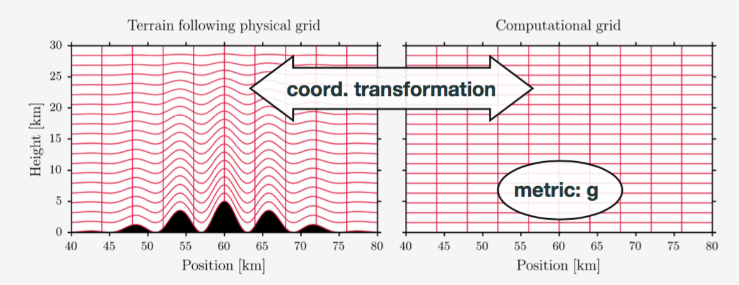

- $h_s = h_s(x,y)$ is the prescribed mountain profile and z_{top} is the top of the model domain

$$\zeta = z_{top} \frac{z - h_s}{z_{top} - h_s}, \quad z(\zeta) = h_s(x,y) + \zeta \, \frac{z_{top} - h_s}{z_{top}}; \quad h_s \le z \le z_{top}.$$

- The Jacobian associated with the transform $(x, y, z) \to (x, y, \zeta)$ is

$$\sqrt{G} = \left[\frac{\partial z}{\partial \zeta} \right]_{(x,y)} = 1 - \frac{h_s(x,y)}{z_{top}}$$

Transport Equation in the Transformed Coordinates (x,y,ζ)

- The 3D transport equation (flux-from) for a density ρ in 3D (x,y,ζ) coordinates can be written as:

$$\frac{\partial \rho}{\partial t} + \nabla \cdot \mathbf{F}(\rho) = 0 \quad \Rightarrow \quad \frac{\partial \tilde{\rho}}{\partial t} + \frac{\partial}{\partial x}(\tilde{\rho}\, u) + \frac{\partial}{\partial y}(\tilde{\rho}\, v) + \frac{\partial}{\partial \zeta}(\tilde{\rho}\, \tilde{w}) = 0,$$

  where $\tilde{\rho} = \sqrt{G}\rho$, the Jacobian-weighted density, and $\tilde{w}$ the vertical velocity in transformed coordinates:

$$\tilde{w} = \frac{d\zeta}{dt}, \quad \sqrt{G}\tilde{w} = w + \sqrt{G}G^{13}\, u + \sqrt{G}G^{23}\, v,$$

  with the metric coefficients (*Clark 1977, JCP*)

$$\sqrt{G}G^{13} \equiv \left[\frac{\partial h_s}{\partial x}\right]_{(z)} \left(\frac{\zeta}{z_{top}} - 1\right), \quad \sqrt{G}G^{23} \equiv \left[\frac{\partial h_s}{\partial y}\right]_{(z)} \left(\frac{\zeta}{z_{top}} - 1\right).$$

- For the '2D + 1D' split case:

$$\frac{\partial \tilde{\rho}}{\partial t} + \frac{\partial}{\partial x}(\tilde{\rho}\, u) + \frac{\partial}{\partial y}(\tilde{\rho}\, v) = -\frac{\partial}{\partial \zeta}(\tilde{\rho}\, \tilde{w})$$

Numerical Expt: Flow over a 3D Schär-type mountain

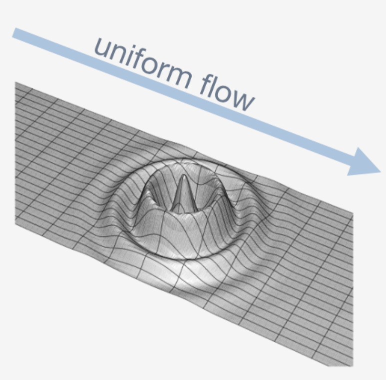

Mountain profile $h_s(x,y)$

- Physical domain: 120 km $\times$ 30 km $\times$ 30 km
- Solid-body rotation in a channel with $u = 20$ m/s, $v = 0$ and $w = 0$.
- BC: Lateral - Periodic; Top/Bottom - No-flux
- Mountain height $h_0 = 5$ km
- Mountain profile:

$$h_s(x,y) = h_0 \exp(-(r/a_0)^2) \cos^2(\pi r/b_0),$$

radial distance $r = \sqrt{(x-x_0)^2 + (y-y_0)^2}$, $a_0 = 10$ km, $b_0 = 6$ km;

- Period for one revolution $t = 6000$ s.
- Initial tracer value centered at $\mathbf{x}_0 = (x_0, y_0, z_0)$, with $d = |\mathbf{x} - \mathbf{x}_0|$

$$\rho(\mathbf{x}) = a \cos^2(d\pi/2), \text{ if } d \leq 1$$
$$= 0, \quad \text{otherwise}$$

- DG simulations with full 3D and split 2D+1D. Starting with $32 \times 8 \times 8$ elements, and 4^3 GLL points on each element.

Flow over a Mountain Test

- Virtually identical results with 3D and split 2D+1D tests

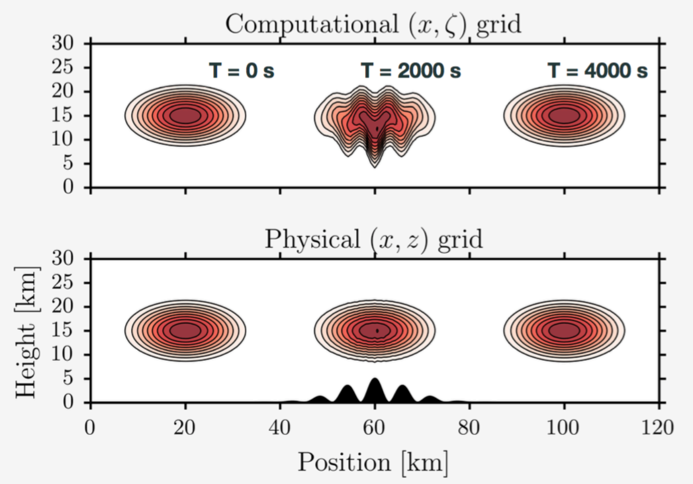

Figure: Positions of the cosine blob as a function of time

Flow over a Mountain Test: h Convergences

- 3D and split DG results are very close
- Reduced convergence rate may be due to evolving the Jacobian-weighted scalar $(\rho\sqrt{G})$.

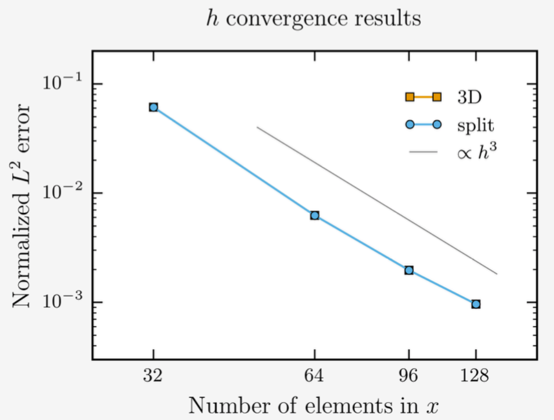

Idealized Non-Hydrostatic Atmospheric Model: [3D Euler System]

- The compressible Euler system can be written in 3D Cartesian (x, y, z) coordinates:

$$
\begin{aligned}
\frac{\partial \rho}{\partial t} + \nabla \cdot (\rho \mathbf{u}) &= 0 \\
\frac{\partial \rho \mathbf{u}}{\partial t} + \nabla \cdot (\rho \mathbf{u} \otimes \mathbf{u} + p\mathbf{I}) &= -\rho g \mathbf{k} \\
\frac{\partial \rho \theta}{\partial t} + \nabla \cdot (\rho \theta \mathbf{u}) &= 0
\end{aligned}
$$

- ρ is the air density, $\mathbf{u} = (u, v, w)$ the velocity vector and is θ the potential temperature, and p is the pressure.
- The pressure p and θ are related through the equation of state:

$$
p = p_0 \left(\frac{\rho \theta R_d}{p_0} \right)^{c_p/c_v} ; \; p_0 = 10^5 \mathrm{Pa},
$$

- Split the variables $\psi = \overline{\psi} + \psi'$, $\psi \in \{\rho, \theta, \rho\theta, p\}$, about the mean hydrostatic state.

- Computational form: Removing the hydrostatically balanced $(d\overline{p}/dz = -\overline{\rho} g)$ reference state from the Euler system yields the perturbation form:

$$
\frac{\partial}{\partial t}\begin{bmatrix} \rho' \\ \rho u \\ \rho v \\ \rho w \\ (\rho\theta)' \end{bmatrix} + \frac{\partial}{\partial x}\begin{bmatrix} \rho u \\ \rho u^2 + p' \\ \rho uv \\ \rho uw \\ \rho u\theta \end{bmatrix} + \frac{\partial}{\partial y}\begin{bmatrix} \rho v \\ \rho vu \\ \rho v^2 + p' \\ \rho vw \\ \rho v\theta \end{bmatrix} + \frac{\partial}{\partial z}\begin{bmatrix} \rho w \\ \rho wu \\ \rho wv \\ \rho w^2 + p' \\ \rho w\theta \end{bmatrix} = \begin{bmatrix} 0 \\ 0 \\ 0 \\ -\rho' g \\ 0 \end{bmatrix}.
$$

NH3D: 3D Non-hydrostatic Gravity Waves

- 3D extension of the Inertia-Gravity Wave (IGW) test (*Skamarock & Klemp, 1994*)

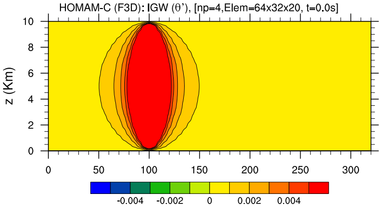

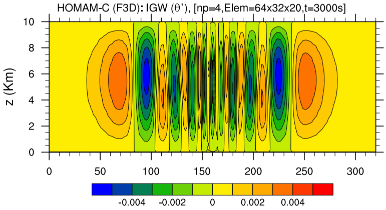

Potential temperature perturbation (θ') in x-z plane

- Evolution of potential temperature perturbation (θ') in a uniform mean flow with a stratified atmosphere.
- Physical domain: 320 km $\times$ 160 km $\times$ 10 km
- $u = 20$ m/s, $v = 0$ and $w = 0$.
- BC: Lateral - Periodic; Top/Bottom - No-flux
- IGW is triggered by perturbing $\theta = \theta_0 + \theta'$:

$$\theta'(x,y,z) = \frac{a^2 \sin(\pi z/z_t)}{a^2 + (x - x_c)^2 + (y - y_c)^2}$$

  where $\theta_0 = 300$K, $a = 5$ km, $z_t = 10$ km, $x_c = 100$ km, $y_c = 80$ km.
- Period of simulation $t = 3000$ s.

IGW θ' Convergence: Split vs. Full 3D

- Difference (Full3D – Split 2D+1D) field (θ')

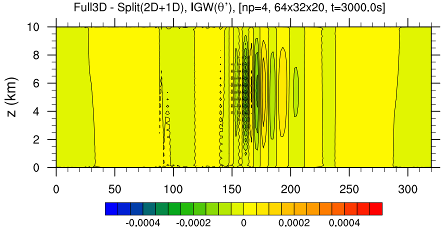

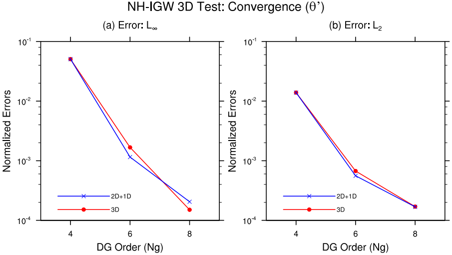

Reference solution is computed with 10^{th}-order DG scheme on $64 \times 32 \times 8$ elements

NH3d: Steady-State Test

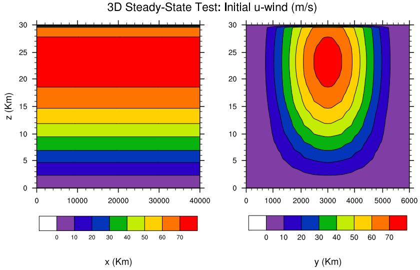

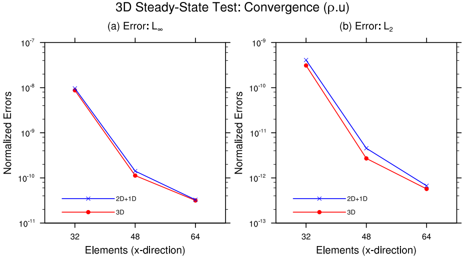

- A modified version of the steady-state test (*Ullrich & Jablonowski (MWR, 2012)*)
- Geostrophically balanced initial conditions, f-plane approximation. $t = 3600$s
- Physical domain: $L_x \times L_y \times L_z$ channel, $L_x = 40,000$ km, $L_y = 6,000$ km, $L_z = 30$ km.
- Initial velocity $v = w = 0$,

$$u(x, y, \eta) = -35 \sin^2\left(\frac{\pi y}{L_y}\right) \ln \eta \, \exp\left[-\frac{(\ln \eta)^2}{25}\right]$$

$$\eta = p/p_s, \quad u(x, y, \eta) \Rightarrow u(x, y, z)$$

- The "analytic solution" is the initial condition.
- The error characteristics of 3D and the split 2D+1D models are very close.

Summary

To assess the Dimensional Splitting errors in 3D-DG Atmospheric Model

- Non-Hydrostatic DG models based on full-3D and dimension-split (2D+1D) spatial discretization have been developed in Cartesian geometry.
- Time integration is performed with explicit SSP RK method
- Both models recover expected convergence rate for smooth 3D advection problems
- In terms of accuracy and convergence, both models found to be virtually identical for several test cases.
- The 2D+1D split approach is promising in 3D atmospheric modeling, also it is slightly more computationally efficient ($\approx 10\%$) than full-3D.

Future Research:

- Compare full-3D and split cases with practical IMEX or semi-implicit time integration methods
- Compare the accuracy of the vertical discretization for split 2D+1D case and 2D + VLC (Vertical Lagrangian Coordinates)

Thank You!